

DiGNet: Learning Scalable Self-Driving Policies for Generic Traffic Scenarios with Graph Neural Networks

Peide Cai, Hengli Wang, Yuxiang Sun, and Ming Liu, *Senior Member, IEEE*

Abstract—Traditional modular self-driving frameworks scale poorly in new scenarios, which usually require tedious hand-tuning of rules and parameters to maintain acceptable performance in all foreseeable occasions. Therefore, robust and safe self-driving using traditional frameworks is still challenging, especially in complex and dynamic environments. Recently, deep-learning based self-driving methods have shown promising results with better generalization capability but less hand engineering effort. However, most of the previous learning-based methods are trained and evaluated in limited driving scenarios with scattered tasks, such as lane-following, autonomous braking, and conditional driving. In this paper, we propose a graph-based deep network to achieve scalable self-driving that can handle massive traffic scenarios. Specifically, more than 7,000 km of evaluation is conducted in a high-fidelity driving simulator, in which our method can obey the traffic rules and safely navigate the vehicle in a large variety of urban, rural, and highway environments, including unprotected left turns, narrow roads, roundabouts, and pedestrian-rich intersections. The results also show that our method achieves better performance over the baselines in terms of success rate. This work is accompanied with some demonstration videos which are available at: <https://sites.google.com/view/dignet-self-driving/video-clips/>.

I. INTRODUCTION

Decision, planning and control for self-driving vehicles (SDVs) in complex and dynamic traffic scenarios are quite challenging. For one thing, there are diverse road topologies, geometries and scenarios (e.g., roundabouts, multi-lane streets and intersections) to consider [1]. For another, the complex and coupled interaction among multiple road agents (e.g., pedestrians, bicyclists and vehicles) are hard to model [2]. Besides these, various traffic rules should also be obeyed, such as traffic light, lane markings and speed limit.

Classical methods use priors and domain knowledge to decompose the self-driving task into a modular and sequential pipeline [3], [4], which consists of perception, planning and control. However, the main drawback of these approaches is the difficulty to generalize in new scenarios, thus they require time-intensive and iterative hand tuning of rules and parameters to maintain performance [5]. Further common problems are the occurrence of local minima [6] and oscillations [7]. In recent years, as an alternative way, deep learning has advanced the SDV technology to a great extent. The ability to

This work was supported by the National Natural Science Foundation of China, under grant No. U1713211, Collaborative Research Fund by Research Grants Council Hong Kong, under Project No. C4063-18G, and HKUST-SJTU Joint Research Collaboration Fund, under project SJTU20EG03, awarded to Prof. Ming Liu. (Corresponding author: Ming Liu.)

All authors are with The Hong Kong University of Science and Technology (email: {pcaiaa,hwangdf,ceyxsun,eelium}@ust.hk).

learn and self-optimize its behavior from data makes a deep driving model well suited to decision and control problems in high-dimensional, nonlinear and dynamic environments [8]–[14], which is free from the laborious engineering maintenance that requires explicit modeling of all foreseeable scenarios. However, current learning models have not been well designed for scalable self-driving in a uniform setup. Specifically, most works only focus on scattered tasks such as conditional urban driving [10]–[14], lane-following [15], [16], lane-changing [17] or collision avoidance [18]–[21]. In short, high-performance scalable driving models that can handle massive traffic scenarios still seem out of reach.

In order to solve the above problem, in this paper we propose a graph-based deep neural network *DiGNet* (driving in graphs) for scalable self-driving. Specifically, we use graph attention networks (GAT) [22] to model the complex interactions among traffic agents, use semantic bird’s-eye view (BEV) images to model road topologies and traffic rules, and adopt the variational auto-encoder (VAE) [23] to extract compact yet effective environmental features. The main contributions of this paper are as follows.

- We propose a specially designed network architecture for self-driving in generic traffic environments, which considers both traffic rules (e.g., speed limit and traffic light) and interaction among multiple dynamic road agents (e.g., collision avoidance at the vehicle- and pedestrian-rich intersections).
- We demonstrate the scalable and safe self-driving performance of the proposed method through extensive closed-loop evaluation in both seen and unseen urban/rural/highway environments.

II. RELATED WORK

A. End-to-End Self-Driving

With the powerful representation capabilities of deep neural networks, *end-to-end* driving approaches [9]–[16] directly take as input the raw sensor readings (e.g., LiDAR point clouds, camera images) to output control commands such as steering angle and throttle. These methods are mostly trained with imitation learning where the agent tries to mimic an expert driver. During training, the deep network compares the action error between its prediction and the expert labelled data, then adjust its weights using gradient descent. For example, based on large amount of labelled data, Xu *et al.* [16] developed an end-to-end architecture to predict future vehicle egomotions. However, this work only targets lane-following tasks and lacks closed-loop experiments. Codevilla *et al.* [12] propose a conditional imitation learning approach

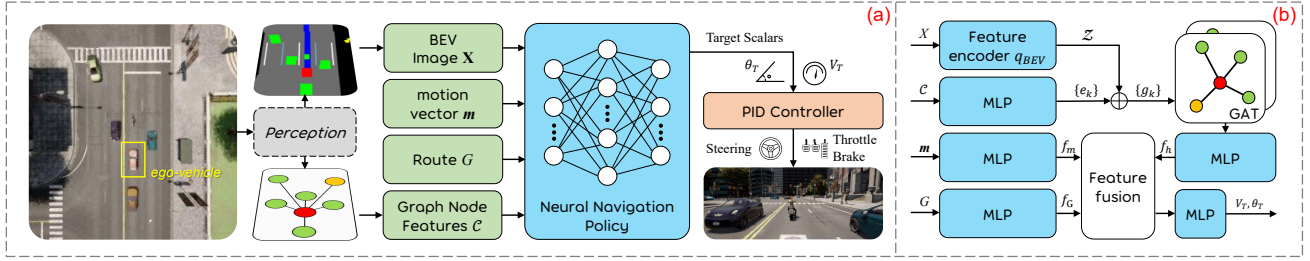


Fig. 1. (a) Schematic overview of the proposed method for self-driving. (b) The data flow inside the neural navigation network (DiGNet). In this work, we assume the input information is accessible with a functioning perception module, and focus on *learning to act* of SDVs.

that splits the network into multiple branches for discrete tasks such as *follow lane* and *turn left/right*. Follow-up works include [10], [13] and [14]. However, these methods cannot handle complex road topologies such as multi-lane streets or roundabouts. Recently, Cai *et al.* [9] use global routes as direction to achieve robust end-to-end navigation in complex dynamic environments with multi-modal sensor fusion. The drawback of this work is the neglect of both traffic rules and efficient interaction with other road agents (e.g., bypassing a vehicle blocked ahead). Another training pipeline is reinforcement learning (RL) [15], [24], where the agent gains driving knowledge by trial and error aiming to maximize the sum of expected future rewards. However, RL is quite sample inefficient, which means the agent may fail millions of times to derive a good policy. Therefore, it is costly to be used for safety-critical tasks and seldom validated in complex driving scenarios.

To summarize, it is quite challenging to learn a direct mapping from high dimensional sensory observations to low dimensional control output, as the end-to-end approaches conflates two aspects of driving: *learning to see* and *learning to act*. Therefore, they suffer from the inherent domain gap problem [25], which prevents them from scalable self-driving (demonstrated in Sec. V).

B. Learning to Drive by Semantic Abstraction

To alleviate the above problem, recently, there arises another framework that uses *semantic* perception results to learn driving policies (e.g., HD maps [1], [26], birdseye views (BEVs) of the surroundings [27], and occupancy maps [28]). Compared with the redundant sensory observations, these semantic input representations are both concise and informative, and have better environmental consistency. These properties help the training process focuses on *learning to act*, which is more efficient and generalizable. For example, the policy network of [28] takes as input hybrid features composed of roadmap, traffic light, route plans and dynamic objects to produce waypoints to follow. This has the advantage to help the network learn meaningful contextual cues behind the human driver's action and achieve more complex driving behaviors. However, [28] mainly shows its results on offline *logged data*, and only performs closed-loop evaluation in simple environments with at most 2 obstacles. Such problem also exists in other similar works [26], [27]. According to [13], the driving performance can vary a lot

between offline open-loop tests and online closed-loop tests, where only the latter can reveal the actual performance. In this work, our input representation is similar to that of [26]–[28] but differently, we focus more on dynamic, interactive and large-scale *closed-loop* driving performance.

C. Graph Representation Learning

Many real-world problems can be modeled with graphs where the nodes contain features of different entities, and edges represent interactions between entities. A challenge in learning on graphs is to find an effective way to get a meaningful aggregated feature representation to facilitate downstream tasks. Recently, graph convolutional networks (GCNs) [29] have shown to be effective in many applications such as social networks, personalized recommendation and link prediction. GCN generalizes the 2D convolution on grids to graph-structured data. When training a GCN, a fixed adjacency matrix is commonly adopted to aggregate feature information of neighboring nodes. On the other hand, graph attention network (GAT) [22] is a GCN variant which aggregates node information with weights learned in a self-attention mechanism. Such adaptiveness of GAT makes it more effective than GCN in graph representation learning.

Recently, these graph neural networks (GNNs) have also been shown to be effective in robotics such as crowd robot navigation [2], [30], where the robot can navigate safely in human crowds with various sizes. However, these works totally neglect the environmental structures, which is not that important for indoor robot navigation in restricted areas, but is non-negligible for outdoor self-driving problems where traffic rules should be strictly obeyed, such as driving on correct lanes. In this work, we borrow the idea of GNN to model the traffic scenes as graphs and use a context-aware GAT to achieve autonomous vehicle navigation.

III. FORMULATION

Fig. 1 shows the structure of the proposed DiGNet for scalable self-driving. The goal is to drive safely and efficiently in a large variety of complex and dynamic outdoor environments for point-to-point navigation. To this end, we use GAT to model the complicated interactions among road agents, and BEV images to represent various road structures. In addition, our system is trained and evaluated in the open-source CARLA simulation (0.9.9) [31], since it possesses abundant vehicle models and maps close to the real world.

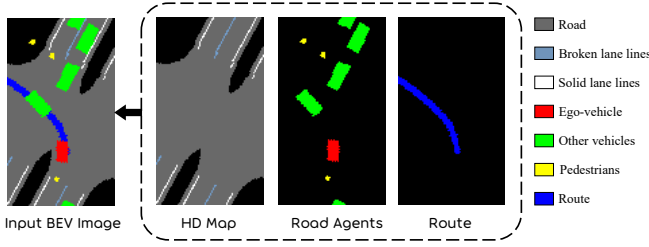


Fig. 2. BEV representation as one of the input to our network, which includes information of HD map, road agents, routes and traffic light.

A. Driving Scene Representation

In order to learn good driving policies, we use semantic BEV images as the representation of driving scenes to reduce the high-dimensionality and redundancy of raw sensory data. Furthermore, with such representation, there is no domain difference between the simulation and real world, thus the policy transfer problem [32] can be alleviated. Specifically, we rasterize different semantic elements (e.g., lane marking, obstacles) into multiple binary channels to form a concise and informative scene representation. As shown in Fig. 2, our BEV input is composed of the following three parts with seven channels in total:

- **High-definition (HD) Map:** The HD map contains the drivable area and lane markings (solid and broken lines). Leveraging map information to learn driving policies is very helpful because it provides valuable structural priors on the motion of surrounding road agents. For example, vehicles normally drive on lanes rather than on sidewalks. Another benefit is that vehicles need to drive according to traffic rules, such as not crossing solid lane markings.
- **Routes and Traffic Light:** The route is provided by a global planner implemented with A^* . The route channel will be set to blank when the traffic light that effects the ego-vehicle turns to red, otherwise it maintains its normal value.
- **Road Agents:** We render the ego-vehicle, other vehicles and pedestrians in three other channels.

In this work, our region of interest is $W=20$ m wide (10 m to each side of the ego-vehicle) and $H=35$ m long (25 m front and 10 m behind of the ego-vehicle). The image resolution is set to 0.25 m/pixel, which finally results in a binary BEV input \mathbf{X} of size $80 \times 140 \times 7$, which is always anchored at the ego-vehicle's current position.

B. Data Collection

We collect a dataset of 260 expert driving episodes in CARLA, which lasts about 7.6 hours and covers a driving distance of 150 km. For each data collection episode, we set random routes ranging from 300 m to 1500 m in four maps of CARLA: Town03, Town05, Town06 and Town07. These maps includes urban, rural and highway scenarios. We also set roaming pedestrians and vehicles to construct dynamic environments, which are controlled by the AI engine of CARLA to form realistic traffic scenarios¹.

¹https://carla.readthedocs.io/en/latest/adv_traffic_manager/

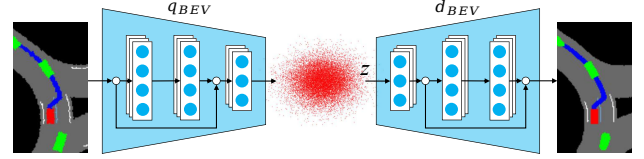


Fig. 3. VAE architecture. The input image is encoded into a latent space, from which the sampled vector \mathbf{z} can be decoded back into a reconstructed image similar to the input. Therefore, \mathbf{z} summarizes the key geometrical properties of environments.

IV. METHODOLOGY

A. Learning the Context Embedding

Although we replace the complex raw sensor data with more informative and concise BEV semantic masks, it is still quite high-dimensionality compared to the vehicle state variables (e.g., speed, location, etc.). Such high-dimensionality makes it not only hard to learn good policies in data scarce tasks, but also suffer from over-fitting problems. Therefore, a lower-dimensional embedding for the multi-channel BEV input is needed for us to train a high-performance driving policy. To this end, we first train a variational autoencoder (VAE) on the collected BEV images from Section III-B. As shown in Fig. 3, this method can help to summarize the key geometrical properties of environments in a low-dimensional latent vector \mathbf{z} . More specifically, we adopt the β -VAE [33] and minimize the variational lower bound with encoder q_{BEV} and decoder d_{BEV} :

$$\mathcal{L}_{VAE} = \beta \cdot \text{D}_{KL}(q_{BEV}(\mathbf{z} | \mathbf{X}) || p(\mathbf{z})) + \|d_{BEV}(\mathbf{z}) - \mathbf{X}\|_2^2, \quad (1)$$

where $\text{D}_{KL}(\cdot)$ is the Kullback-Leibler (KL) divergence. The encoder $q_{BEV}(\mathbf{z} | \mathbf{X})$ takes as input the raw image and returns the mean μ and variance σ^2 of a normal distribution, such that $\mathbf{z} \sim \mathcal{N}(\mu, \sigma^2)$. $p(\mathbf{z})$ is the prior on the latent space, modeled as the standard normal distribution $\mathcal{N}(0, I)$. The second term of (1) is the MSE loss between the raw and reconstructed images ($\mathbf{X}, d_{BEV}(\mathbf{z})$). The parameter β provides a trade-off between these two types of losses.

In this work, we set $\beta = 0.01$ and $\mathbf{z} \in \mathbb{R}^{512}$. We implement the VAE based on the ResNet18 architecture [34], where the decoder uses a combination of upsampling and convolutions for image reconstruction. Note the parameters of VAE are fixed during later policy training for stable performance.

B. Graph Modeling of Driving Scenes

1) *Network Architecture:* As shown in Fig. 1, we use GAT to model the interaction among road agents during driving, which is composed of multiple graph layers. The input to the i -th layer is a set of node features, $\{h_1^i, h_2^i, \dots, h_N^i\}$, $h_k^i \in \mathbb{R}^{F^i}$, where N is the number of nodes (agents, including the ego-vehicle), and F^i is the dimension of features in each node. Then, information of each node k are propagated to the neighboring nodes \mathcal{N}_k and being used to update the node features via a self-attention mechanism, which produces the output of the layer:

$$h_k^{i+1} = \sigma\left(\sum_{j \in \mathcal{N}_k} \alpha_{kj}(h_k^i, h_j^i) \mathbf{W} h_j^i\right), \quad (2)$$

where $\sigma(\cdot)$ is the nonlinear activation function, e.g., ReLU; $\mathbf{W} \in \mathbb{R}^{F^{i+1} \times F^i}$ is a shared weight matrix to be applied to each node for expressive feature transformation; $\alpha_{kj}(\cdot, \cdot)$ means the importance of node j to node k , which is the normalized attention coefficients computed with shared weight vector $\tilde{\mathbf{a}} \in \mathbb{R}^{2F^{i+1}}$:

$$\alpha_{kj}(\mathbf{h}_k^i, \mathbf{h}_j^i) = \frac{\exp(\sigma(\tilde{\mathbf{a}}^T [\mathbf{W}\mathbf{h}_k^i \parallel \mathbf{W}\mathbf{h}_j^i]))}{\sum_{m \in \mathcal{S}_k} (\sigma(\tilde{\mathbf{a}}^T [\mathbf{W}\mathbf{h}_k^i \parallel \mathbf{W}\mathbf{h}_m^i]))}, \quad (3)$$

where \parallel represents the concatenation operation. Furthermore, We follow the *multi-head attention* method in [22] to stabilize the learning process. Specifically, S^i independent graph networks execute the transformation of (2) and their features are concatenated to produce the output of the i -th layer:

$$\mathbf{h}_k^{i+1} = \parallel_{s=1}^{S^i} \sigma(\sum_{j \in \mathcal{N}_i} \alpha_{kj}^s(\mathbf{h}_k^i, \mathbf{h}_j^i) \mathbf{W}^s \mathbf{h}_j^i). \quad (4)$$

For the final layer, we employ *averaging* among multiple heads rather than concatenation.

2) *Implementation Details*: In this work, we adopt a two-layer GAT and set $S^1, S^2 = 5$, $F^1, F^2 = 256$. The input features \mathcal{C} include motion state information for each node (road agent) in the ego-vehicle's local coordinate. For node $k \in \{1, 2, \dots, N\}$, the input feature is a 10-dimensional vector:

$$\mathbf{c}_k = \{x, y, d, \psi, vx, vy, ax, ay, w, l\}, \quad (5)$$

which includes its location (x, y) , distance to the ego-vehicle (d) , yaw angle (ψ) , velocity (vx, vy) , acceleration (ax, ay) and size (width w and length l). In the spirit of [2], we first pass each node state $\mathbf{c}_k \in \mathcal{C}$ through a multilayer perceptron (MLP) to produce a feature vector $\mathbf{e}_k \in \mathbb{R}^{128}$ for sufficient expressive power. For context-aware graph modeling, we then concatenate \mathbf{e}_k with \mathbf{z} derived from the VAE introduced in Section IV-A, to generate the mixed vector \mathbf{g}_k . Then the set $\{\mathbf{g}_k\}$ are sent to GAT to output the final aggregated feature $\mathbf{h}_k^o \in \mathbb{R}^{256}$, which represents the internal interactions on each node k . We are interested in the result \mathbf{h}_1^o of the first node, which represents the influence on the ego-vehicle.

C. Task-relevant Feature Embedding

In addition to the interaction feature \mathbf{h}_1^o derived from the above section, we also need task-relevant information of the ego-vehicle to achieve mannered goal-directed self-driving, which is composed of two other feature vectors. The first vector $\mathbf{m} \in \mathbb{R}^{13}$ describes the ego-motion as follows:

$$\mathbf{m} = \{\tau_s, \tau_t, \tau_b, v_{lim}, vx, vy, ax, ay, e_v, e_{cte}, e_{heading}, F_l, F_r\}, \quad (6)$$

where τ_s, τ_t and τ_b indicate the current control command of the ego-vehicle: steering angle, throttle and brake. v_{lim} means the traffic speed limit, e_v means the difference between v_{lim} and current vehicle speed, e_{cte} is the cross track error between the vehicle location and the reference route, and $e_{heading}$ is the heading angle error calculated with vector field guidance [35]. $F_{l(r)}$ is a binary indicator of the lane marking on the left (right) side of the ego-vehicle, which is set to 1

if the lane marking is crossable (e.g., a broken line), and set to 0 otherwise (e.g., a solid line).

The second vector is a route vector $G \in \mathbb{R}^{150}$:

$$G = \{(x_k, y_k) \mid 1 \leq k \leq 75\} \subset G_f, \quad (7)$$

where G_f is the full high-level route from the start point to the destination. During navigation, we down-sample G_f into local relevant route G based on the ego-vehicle's location. Specifically, the first waypoint (x_1, y_1) in G is the closest waypoint in G_f to the current vehicle location, and the distance of every two adjacent points is 0.4 m. Note the redundancy of route information in G and BEV is meaningful, where the state vector here provides more specific waypoint locations for the vehicle to follow, while the route mask of BEV can indicate if there are any obstacles on conflicting lanes of planned routes, as well as encode traffic light information.

Finally, we adopt three MLPs to transform \mathbf{m} , G and \mathbf{h}_1^o separately into feature vectors $f_m, f_G, f_h \in \mathbb{R}^{1024}$ for further processing.

D. Driving Policy Training

With components defined above, the derived feature vectors f_m, f_G, f_h are combined and then processed with a MLP to produce the final output for navigating the vehicle. Different from most of the previous end-to-end driving methods [10]–[14] that directly regress vehicle control commands (e.g., steering and throttle), we adopt a mid-level output representation indicating the target speed v_T and course angle θ_T . For implementation, to bound the range of v_T and θ_T , we regress two scalars of target speed ($\kappa_v \in [0, 1]$) and course angle ($\kappa_\theta \in [-1, 1]$). Then the target control values can be computed as follows:

$$v_T = v_{lim} \times \kappa_v, \quad \theta_T = 90^\circ \times \kappa_\theta. \quad (8)$$

These mid-level indicators are finally translated by a PID controller to generate the device-level control commands, i.e., steering, throttle and brake. In this way, we can reduce the burden of control and inject the information of speed limit to the model output, which leads to more flexible policy models. We use L1 loss in terms of v_T and θ_T to train the policy by imitation learning.

V. EXPERIMENTS AND DISCUSSION

A. Training setup

We train our network DiGNet on the collected dataset introduced in Section III-B. The split ratio of training, validation and testing set is set to 17:1:2, leading to 240K training samples. We set the batch size to 256, and use the Adam optimizer with a learning rate of 0.0001. For comparison, we also train six other baselines, which can be divided into the following two categories:

1) End-to-end self-driving method.

- CILRS. It is one of the state-of-the-art vision-based end-to-end driving method [13], which takes as input the front-facing camera images and vehicle speeds to output

TABLE I

CLOSED-LOOP EVALUATION RESULTS OF DIFFERENT MODELS ON SIX MAPS IN CARLA. SR MEANS THE SUCCESS RATE (%), AND DS MEANS THE DRIVING SCORE. LARGER NUMBERS ARE BETTER. THE BOLD FONT HIGHLIGHTS THE BEST RESULTS IN EACH COLUMN.

Models	Training Towns								Unseen Towns			
	Town03		Town05		Town06		Town07		Town04		Town10	
	<i>urban</i>		<i>urban</i>		<i>highway</i>		<i>rural</i>		<i>mixed</i>		<i>urban</i>	
	SR	DS	SR	DS	SR	DS	SR	DS	SR	DS	SR	DS
CILRS	43.2	0.56	38.2	0.52	35.2	0.48	44.8	0.59	16.2	0.28	1.2	0.11
MLP	62.3	0.72	60.0	0.69	72.2	0.79	75.0	0.82	60.5	0.70	38.2	0.53
GCN (U)	68.8	0.77	70.2	0.78	73.8	0.80	73.0	0.80	68.5	0.76	55.2	0.66
GCN (D)	74.2	0.80	71.5	0.79	74.8	0.81	75.2	0.82	64.0	0.72	62.5	0.71
GAT	76.0	0.82	81.5	0.87	78.2	0.83	76.8	0.83	71.0	0.78	68.0	0.75
DiGNet (CTL)	72.8	0.79	69.8	0.77	73.2	0.79	73.5	0.80	67.5	0.75	49.0	0.58
DiGNet (<i>ours</i>)	80.2	0.85	75.0	0.82	78.2	0.83	80.0	0.85	72.8	0.80	67.2	0.75

control commands. This baseline is added to verify that policies trained with abstracted semantics have better generalization capability.

2) *Graph state*-based methods. These networks are named based on how they process the node features \mathcal{C} .

- GCN (U). It takes as input $\{\mathcal{C}, G, \mathbf{m}\}$ to produce the output, which adopts a two-layer GCN to process the node features \mathcal{C} . We refer to the baseline *U-GCNRL* introduced in [2] and set the adjacency matrix of GCN with uniform weights.
- GCN (D). It is similar to GCN (U) but uses distance-related weights in its adjacency matrix. It adopts a straightforward intuition that obstacles closer to the ego-vehicle should exert a stronger influence. This network follows the idea of *D-GCNRL* introduced in [2].
- GAT. Its difference to our proposed method is the non-use of the context embedding \mathbf{z} .
- DiGNet (CTL). It is a variant of our method utilizing both graph state and context embedding \mathbf{z} . However, it directly generates device-level control commands (i.e., steering, throttle and brake), rather than the mid-level target speed/angle scalars.
- MLP. It uses MLP rather than GNNs to process the node features. This baseline is added to verify the advantage of GNN to handle interactions among different nodes.

B. Evaluation

1) *Benchmark*: In order to cover as many driving scenarios as possible to thoroughly evaluate different methods, we choose the most complicated six maps in CARLA, including two unseen maps Town04 and Town10 for closed-loop driving tasks. Town04 is a mixed environment with highway roads and a small town². More concretely, in each map, we set 10 routes for the ego-vehicle to drive, and each route corresponds to 40 driving episodes. For each episode, we set random number of vehicles (10 ~ 300) and pedestrians (10 ~ 90) navigating around the map, which are also spawned

with random properties (i.e., speeds, destinations) at random positions. Due to such randomness, the environmental dynamics of seen maps is also different from the training dataset. Finally, we conduct 16,800 episodes to evaluate seven driving models, covering a distance of 7,102 km.

Note that compared with previous benchmark methods introduced in [13], [31], ours covers much more traffic scenarios, which is more suitable to evaluate the self-driving performance.

2) *Metrics*: We use two metrics to measure the driving performance on each map. The first is success rate (SR). An episode is considered to be successful if the agent reaches a certain goal without any collision. The episode will be recounted if the agent gets stuck in traffic jam. The second metric is driving score (DS) defined as $\frac{1}{n} \sum_i^n R_i P_i$, where n stands for the number of episodes for each town (400 in this work), R_i is the percentage of completion of the route in the i -th episode, and P_i is the collision penalty of the i -th episode (set to 0.5 if collision happens, otherwise set to 1).

3) *Quantitative Analysis*: Tab. I shows the quantitative evaluation results. For clarity, in the following we list our main findings and corresponding interpretations:

- Semantic scene representations are more suitable than raw sensory data to learn *generalizable* self-driving policies. We can see that the performance drop from seen maps to unseen maps is quite distinct for CILRS. For example, when the testing environment changes from Town03 to Town10, the SR of CILRS significantly drops by 40 times (43.2% \rightarrow 1.2%), while the performance of state-based methods does not degrade that much.

- GNNs are more suitable than MLP to handle interactions among different nodes. As we can see, MLP performs worst among the state-based methods. For example, the SR in Town10 of MLP is only 38.2%, which is much lower than the GNN-based methods (55.2% ~ 68.0%).

- Properly combining both the context and state information can help improve the driving ability, as our method DiGNet achieves the best overall results. We conjecture that the pixel information from the BEVs, which is encoded as the latent vector \mathbf{z} in this work, can provide complementary

²We refer readers to https://carla.readthedocs.io/en/latest/core_map/#carla-maps for more details of these maps.

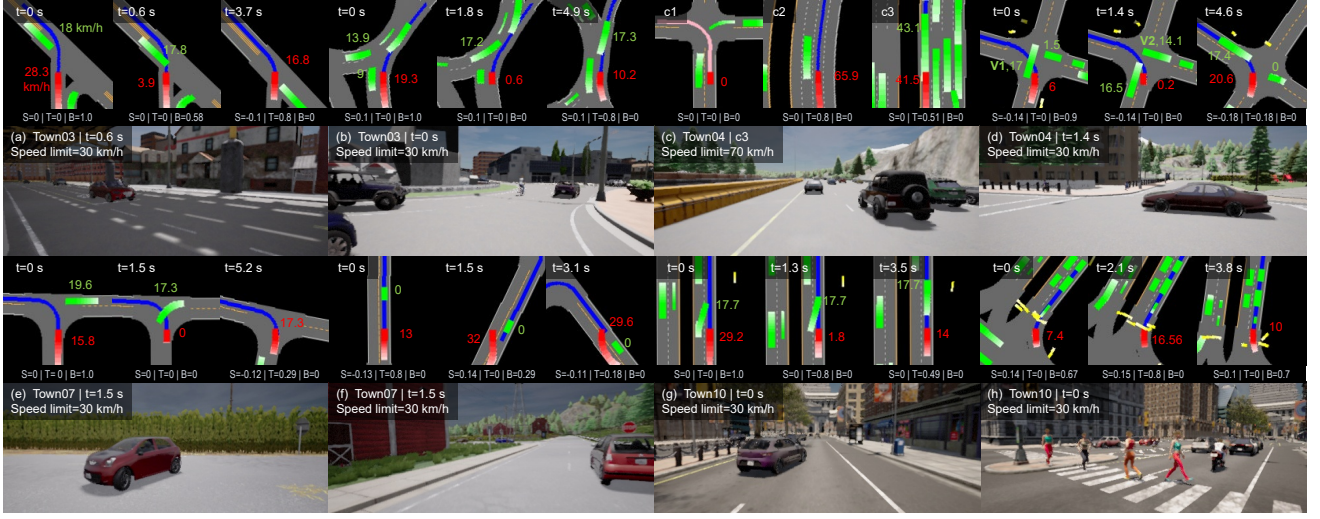


Fig. 4. Closed-loop evaluation results of our DiGNet. We show several driving clips with BEV and FPV images in four maps covering urban, rural and highway areas, where Town04 and Town10 are unseen maps during training. For better visualization, we set the color of route to pink if traffic light turns to red, otherwise to blue. In addition, we render trajectories in the past 1.5 s for road agents, where the lighter color indicates the more distant historical location. We also label the speed of key vehicles (ego-vehicle in red and other vehicles in green), and the output control commands (S-steer, T-throttle, B-brake) for better understanding. The range of steering is $[-1, 1]$, while for throttle and brake the range is $[0, 1]$. The sample driving behaviors are: slowing down when taking unprotected turns at (a,d,e) intersections or (b) roundabouts for collision avoidance, (c1) stopping at intersections with red traffic light, (c2,c3) high-speed driving and vehicle-following on highways, (f) deviating the route a bit to bypass a parked vehicle on narrow roads, (g) timely slowing down when an aggressive vehicle in front suddenly changes lanes to the lane of ego-vehicle, and (h) crowd-aware safe driving behaviors among multiple pedestrians, including slowing down for collision avoidance ($t=0$ s) and continuing to drive when no pedestrians blocking ways ($t=2.1$ s). More demos are shown in our webpage <https://sites.google.com/view/dignet-self-driving/video-clips/>.

spatial features (e.g., road structures and lane positions) on the basis of graph states.

- Using mid-level control outputs (κ_v, κ_θ) rather than direct command signals can achieve better driving results, as DiGNet achieves higher SR and DS than DiGNet (CTL) in all maps.

4) *Qualitative results:* Fig. 4 shows the qualitative results of DiGNet. We can see that our model can safely and efficiently drive in diverse dynamic environments with different road structures (roundabouts, intersections, highways, etc.) and traffic scenarios, whilst obeying traffic rules such as speed limits and traffic lights. For example, in Fig. 4-(d), our model is turning left at an intersection, however, vehicle V1 is coming from the opposite direction without slowing down (speed=17 km/h). Our model timely loses the throttle and applies a large brake (0.9) to avoid collisions. When $t=1.4$ s, another vehicle V2 is coming from the right side at a speed of 14.1 km/h. To avoid collision, our model continues to wait until it is safe to speed up ($t=4.6$ s).

5) *Attention Analysis:* To show the benefits of GAT against other GNN methods in our task, we analyze its attention outputs using Fig. 5. We can see that there is a pedestrian (bounded by the orange box) running across the street in front of the ego-vehicle, which exerts a strong influence with higher attention (0.35) than the other agents (0.04 ~ 0.06), therefore, the ego-vehicle stops at the intersection to avoid an accident by applying a zero throttle value. Note that there is a motorcycle (bounded by green box) at the right lane, which is also very close to the ego-vehicle but assigned with a lower attention (0.06), because it does not have much

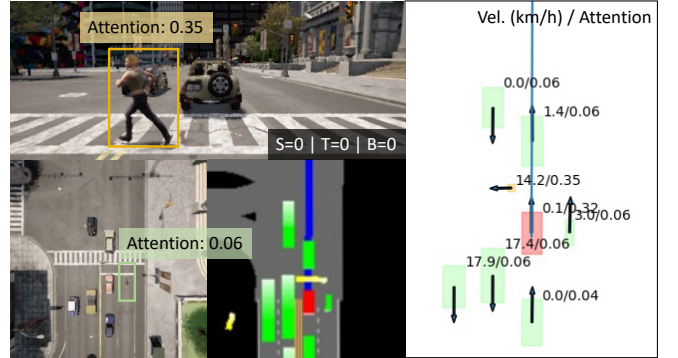


Fig. 5. A sample driving scenario where the ego-vehicle stops for pedestrians with our DiGNet (left). We also show the corresponding attentions for the road agents from the GAT module (right).

influence on the ego-vehicle. This phenomenon demonstrates that the ideas of GCN (U) and GCN (D) are not reasonable in some occasions, because the influences of road agents are not always equal or related with distance. By contrast, GAT is more suitable in our task, which dynamically assigns attentions using a self-attention mechanism based on specific driving contexts. Such difference also explains why GCN methods generally produce worse results than GAT in Tab. I.

VI. CONCLUSION AND FUTURE WORK

In this work we developed a context-aware graph-based deep navigation network named DiGNet to achieve scalable self-driving in generic traffic scenarios, such as unprotected left turns, narrow roads, roundabouts, pedestrian- and vehicle-rich intersections. We showed that decoupling the two parts of previous end-to-end driving methods, i.e.,

learning to see and learning to act, can achieve much better generalization performance in new environments.

More specifically, we first used VAE to encode semantic driving contexts into concise and informative latent vectors, which can then be incorporated with the state information (e.g., locations and speeds) into GNNs to model the complex interactions among road agents. The large-scale closed-loop evaluation results revealed that our method achieves the highest success rates and driving scores in most environments, indicating it can properly complement the context and state information to handle complex driving situations.

In this work, we assumed perfect perception results from the simulator to learn driving policies, which, however, is hard to guarantee in real-world applications in terms of detection errors, occlusion issues and sensor failures. In the future, we will investigate how to learn driving policies with imperfect perception modules.

REFERENCES

- [1] J. Chen, B. Yuan, and M. Tomizuka, "Deep imitation learning for autonomous driving in generic urban scenarios with enhanced safety," *2019 IEEE/RSJ International Conference on Intelligent Robots and Systems (IROS)*, pp. 2884–2890, 2019.
- [2] Y. Chen, C. Liu, B. Shi, and M. Liu, "Robot navigation in crowds by graph convolutional networks with attention learned from human gaze," *IEEE Robotics and Automation Letters*, vol. 5, pp. 2754–2761, 2020.
- [3] J. Leonard *et al.*, "A perception-driven autonomous urban vehicle," *J. Field Robot.*, vol. 25, no. 10, pp. 727–774, 2008.
- [4] E. D. Dickmanns, "The development of machine vision for road vehicles in the last decade," in *Intelligent Vehicle Symposium, 2002. IEEE*, vol. 1. IEEE, 2002, pp. 268–281.
- [5] W. Zeng, W. Luo, S. Suo, A. Sadat, B. Yang, S. Casas, and R. Urtasun, "End-to-end interpretable neural motion planner," *2019 IEEE/CVF Conference on Computer Vision and Pattern Recognition (CVPR)*, pp. 8652–8661, 2019.
- [6] Y. Koren and J. Borenstein, "Potential field methods and their inherent limitations for mobile robot navigation," *Proceedings. 1991 IEEE International Conference on Robotics and Automation*, pp. 1398–1404 vol.2, 1991.
- [7] O. Khatib, "Real-time obstacle avoidance for manipulators and mobile robots," *Proceedings. 1985 IEEE International Conference on Robotics and Automation*, vol. 2, pp. 500–505, 1985.
- [8] S. Kuutti, R. Bowden, Y. Jin, P. Barber, and S. Fallah, "A survey of deep learning applications to autonomous vehicle control," *IEEE Transactions on Intelligent Transportation Systems*, pp. 1–22, 2020.
- [9] P. Cai, S. Wang, Y. Sun, and M. Liu, "Probabilistic end-to-end vehicle navigation in complex dynamic environments with multimodal sensor fusion," *IEEE Robotics and Automation Letters*, vol. 5, pp. 4218–4224, 2020.
- [10] D. Chen, B. Zhou, V. Koltun, and P. Krähenbühl, "Learning by cheating," in *CoRL*, 2019.
- [11] E. Ohn-Bar, A. Prakash, A. Behl, K. Chitta, and A. Geiger, "Learning situational driving," *2020 IEEE/CVF Conference on Computer Vision and Pattern Recognition (CVPR)*, pp. 11 293–11 302, 2020.
- [12] F. Codevilla, M. Miiller, A. López, V. Koltun, and A. Dosovitskiy, "End-to-end driving via conditional imitation learning," in *2018 IEEE International Conference on Robotics and Automation (ICRA)*. IEEE, 2018, pp. 1–9.
- [13] F. Codevilla, E. Santana, A. M. López, and A. Gaidon, "Exploring the limitations of behavior cloning for autonomous driving," in *Proceedings of the IEEE International Conference on Computer Vision*, 2019, pp. 9329–9338.
- [14] L. Tai, P. Yun, Y. Chen, C. Liu, H. Ye, and M. Liu, "Visual-based autonomous driving deployment from a stochastic and uncertainty-aware perspective," *2019 IEEE/RSJ International Conference on Intelligent Robots and Systems (IROS)*, pp. 2622–2628, 2019.
- [15] A. Kendall, J. Hawke, D. Janz, P. Mazur, D. Reda, J.-M. Allen, V.-D. Lam, A. Bewley, and A. Shah, "Learning to drive in a day," *2019 International Conference on Robotics and Automation (ICRA)*, pp. 8248–8254, 2019.
- [16] H. Xu, Y. Gao, F. Yu, and T. Darrell, "End-to-end learning of driving models from large-scale video datasets," *2017 IEEE Conference on Computer Vision and Pattern Recognition (CVPR)*, pp. 3530–3538, 2017.
- [17] P. Wang, C.-Y. Chan, and A. D. L. Fortelle, "A reinforcement learning based approach for automated lane change maneuvers," *2018 IEEE Intelligent Vehicles Symposium (IV)*, pp. 1379–1384, 2018.
- [18] H. Porav and P. Newman, "Imminent collision mitigation with reinforcement learning and vision," *2018 21st International Conference on Intelligent Transportation Systems (ITSC)*, pp. 958–964, 2018.
- [19] Z. Cao, E. Biyik, W. Z. Wang, A. Raventos, A. Gaidon, G. Rosman, and D. Sadigh, "Reinforcement learning based control of imitative policies for near-accident driving," *ArXiv*, vol. abs/2007.00178, 2020.
- [20] H. Chae, C. M. Kang, B. Kim, J. Kim, C. C. Chung, and J. W. Choi, "Autonomous braking system via deep reinforcement learning," in *2017 IEEE 20th International Conference on Intelligent Transportation Systems (ITSC)*. IEEE, 2017, pp. 1–6.
- [21] J. Woo and N. Kim, "Collision avoidance for an unmanned surface vehicle using deep reinforcement learning," *Ocean Engineering*, vol. 199, p. 107001, 2020.
- [22] P. Veličković, G. Cucurull, A. Casanova, A. Romero, P. Liò, and Y. Bengio, "Graph Attention Networks," *International Conference on Learning Representations*, 2018.
- [23] D. P. Kingma and M. Welling, "Auto-encoding variational bayes," in *ICLR*, Y. Bengio and Y. LeCun, Eds., 2014.
- [24] P. Cai, X. Mei, L. Tai, Y. Sun, and M. Liu, "High-speed autonomous drifting with deep reinforcement learning," *IEEE Robotics and Automation Letters*, vol. 5, pp. 1247–1254, 2020.
- [25] J. Zhang, L. Tai, P. Yun, Y. Xiong, M. Liu, J. Boedecker, and W. Burgard, "Vr-goggles for robots: Real-to-sim domain adaptation for visual control," *IEEE Robotics and Automation Letters*, vol. 4, pp. 1148–1155, 2019.
- [26] W. Zeng, S. Wang, R. Liao, Y. Chen, B. Yang, and R. Urtasun, "Dsdnet: Deep structured self-driving network," in *Proceedings of the European Conference on Computer Vision (ECCV)*, 2020.
- [27] M. Bansal, A. Krizhevsky, and A. Ogale, "Chauffeurnet: Learning to drive by imitating the best and synthesizing the worst," in *Proc. Robot.: Sci. Syst.*, June 2019.
- [28] A. Sadat, S. Casas, M. Ren, X. Wu, P. Dhawan, and R. Urtasun, "Perceive, predict, and plan: Safe motion planning through interpretable semantic representations," in *Proceedings of the European Conference on Computer Vision (ECCV)*, 2020.
- [29] M. Defferrard, X. Bresson, and P. Vandergheynst, "Convolutional neural networks on graphs with fast localized spectral filtering," in *NIPS*, 2016.
- [30] L. Manso, R. R. Jorvekar, D. R. Faria, P. Bustos, and P. Bachiller, "Graph neural networks for human-aware social navigation," *ArXiv*, vol. abs/1909.09003, 2019.
- [31] A. Dosovitskiy, G. Ros, F. Codevilla, A. Lopez, and V. Koltun, "CARLA: An open urban driving simulator," in *Proc. 1st Annu. Conf. Robot Learn.*, vol. 78, Nov 2017, pp. 1–16.
- [32] J. Zhang, L. Tai, P. Yun, Y. Xiong, M. Liu, J. Boedecker, and W. Burgard, "Vr-goggles for robots: Real-to-sim domain adaptation for visual control," *IEEE Robotics and Automation Letters*, vol. 4, no. 2, pp. 1148–1155, 2019.
- [33] I. Higgins, L. Matthey, A. Pal, C. Burgess, X. Glorot, M. Botvinick, S. Mohamed, and A. Lerchner, "beta-vae: Learning basic visual concepts with a constrained variational framework," in *ICLR*, 2017.
- [34] K. He, X. Zhang, S. Ren, and J. Sun, "Deep residual learning for image recognition," *2016 IEEE Conference on Computer Vision and Pattern Recognition (CVPR)*, pp. 770–778, 2016.
- [35] D. Nelson, D. B. Barber, T. McLain, and R. Beard, "Vector field path following for miniature air vehicles," *IEEE Transactions on Robotics*, vol. 23, pp. 519–529, 2007.